JACC: CARDIOVASCULAR IMAGING VOL. 11, NO. 2, 2018

PUBLISHED BY ELSEVIER

MRI-Derived Myocardial Strain Measures in Normal Subjects

Ha Q. Vo, MSc,[a] Thomas H. Marwick, MBBS, PhD, MPH,[a,b] Kazuaki Negishi, MD, PhD[a]

ABSTRACT

OBJECTIVES The aim of this study was to perform a systematic review and meta-analysis to estimate the normal ranges of magnetic resonance imaging (MRI)-based feature tracking (FT) and to identify sources of variations. Similar analyses were also performed for strain encoding, displacement encoding with stimulated echoes, and myocardial tagging.

BACKGROUND MRI-FT is a novel technique for quantification of myocardial deformation using MRI cine images. However, the reported 95% confidence intervals (CIs) from the 2 largest studies have no overlaps.

METHODS Four databases (EMBASE, SCOPUS, PUBMED, and Web of Science) were systematically searched for MRI strains of the left (LV) and right (RV) ventricles. The key terms for MRI-FT were "tissue tracking," "feature tracking," "cardiac magnetic resonance," "cardiac MRI," "CMR," and "strain." A random effects model was used to pool LV global longitudinal strain (GLS), global circumferential strain (GCS), global radial strain (GRS), and RVGLS. Meta-regressions were used to identify the sources of variations.

RESULTS 659 healthy subjects were included from 18 papers for MRI-FT. Pooled mean of LVGLS was −20.1% (95% CI: −20.9% to −19.3%), LVGCS −23% (95% CI: −24.3% to −21.7%), LVGRS 34.1% (95% CI: 28.5% to 39.7%), and RVGLS −21.8% (95% CI: −23.3% to −20.2%). Although there were no publication biases except for LVGCS, significant heterogeneities were found. Meta-regression showed that variation of LVGCS was associated with field strength ($\beta = 3.2$; $p = 0.041$). Variations of LVGLS, LVGRS, and RVGLS were not associated with any of age, sex, software, field strength, sequence, LV ejection fraction, or LV size. LVGCS seems the most robust in MRI-FT. Among the MRI-derived strain techniques, the normal ranges were mostly concordant in LVGLS and LVGCS but varied substantially in LVGRS and RVGLS.

CONCLUSIONS The pooled means of 4 MRI-derived myocardial strain methods in normal subjects are demonstrated. Differences in field strength were attributed to variations of LVGCS. (J Am Coll Cardiol Img 2018;11:196-205)

Cardiac wall motion analysis plays a central role for assessment of ventricular contractile function. Cardiac magnetic resonance (CMR) is a radiation-free, reference standard for assessment of cardiac anatomy and wall motion because of its excellent endocardial border definition due to high spatial and contrast resolution. However, the current assessment of wall motion is primarily subjective, and results are skill and experience dependent. The quantification of myocardial deformation provides further insights into cardiac function in a variety of subclinical cardiac diseases (1,2). Although several quantitative assessment techniques have been proposed, such as myocardial tagging (MT), phase contrast velocity imaging, displacement encoding (DENSE), and strain encoding (SENC) for strain analysis (3,4), these methods require additional sequences and time.

Recently, magnetic resonance imaging (MRI) feature tracking (MRI-FT) has been introduced using cine images and provides a fast and accurate assessment of both ventricular (5-12) and atrial strains

From the [a]Menzies Institute for Medical Research, University of Tasmania, Hobart, Tasmania, Australia; and the [b]Baker IDI Heart and Diabetes Institute, Melbourne, Victoria, Australia. Dr. Negishi is supported by an award from the Select Foundation, which had no role in the preparation of this paper. The authors have reported that they have no relationships relevant to the contents of this paper to disclose. Raymond Kim, MD, served as the Guest Editor for this paper.

Manuscript received September 29, 2016; revised manuscript received December 6, 2016, accepted December 9, 2016.

ISSN 1936-878X/$36.00 http://dx.doi.org/10.1016/j.jcmg.2016.12.025

(13,14) with speckle tracking echocardiography (STE) or MT (15). To date, however, only a few data exist on MRI-FT normal reference values, and they are based on small or modest sample-size studies. The reported 95% confidence intervals (CIs) from the 2 largest MRI-FT studies have no overlaps (16,17). Therefore, in this study, we aimed to: 1) perform a systematic review for studies that reported MRI-FT strain values from a normal healthy population; 2) estimate the pooled means of their myocardial strains by meta-analysis; and 3) elucidate possible sources of variation affecting the strain values by meta-regression analyses. We also performed the same systematic review and meta-analysis for DENSE, SENC, and MT.

METHODS

SEARCH STRATEGY. We followed the PRISMA (Preferred Reporting Items for Systematic reviews and Meta-Analysis) guideline when performing our systematic review and meta-analysis (18). The first search was performed on 4 August 2015, and the last search was performed on 21 October 2015. Four databases (EMBASE, PUBMED, Scopus, and Web of Science) were systematically searched for the strain values of the left ventricle (LV) or right ventricle (RV) derived from the MRI-FT technique by 2 coauthors (H.Q.V. and K.N.) under the guidance of a librarian trained in systematic review. The key terms were "tissue tracking," "feature tracking," "cardiac magnetic resonance," "cardiac MRI," "CMR," and "strain." The reference lists of these articles were also scrutinized to identify some additional appropriate studies. Search hedges created are listed in Online Appendix A. The study was prospectively registered with the PROSPERO database of systematic reviews (Normal Ranges of Bi-Ventricular Strain by MRI Feature Tracking: A Systematic Review and Meta-Analysis; CRD42015025616). Methods for DENSE, SENC, and MT are reported in Online Appendices B and C.

SEE PAGE 206

STUDY SELECTION. From these lists, studies were included if the articles reported strain values using cardiac MRI in healthy subjects. The 2 coauthors reviewed and chose studies if the studies met each of following criteria: 1) studies recruited extensively normal healthy subjects; and 2) studies included a control group, which was defined as normal and healthy. The definition of the normal healthy group varies with the studies. In this meta-analysis, this group of subjects was identified if subjects: 1) were not associated with any disease (diabetes, heart failure, and so on) or with overt symptoms or adverse outcomes; 2) did not have any history of heart disease; 3) were not currently implanted with any cardiac devices; 4) were indicated as being healthy; and 5) were >18 years of age. The definitions of healthy subjects are shown in Online Table S1. All discrepancies were reviewed and resolved by consensus of all authors.

STUDY EXCLUSION. The search was uniquely concentrated on human studies, published in English. Animal studies and conference presentations were excluded.

DATA COLLATION. Strain data were extracted from individual studies and entered into an electronic database. Left ventricular global longitudinal strain (LVGLS), left ventricular global circumferential strain (LVGCS), left ventricular global radial strain (LVGRS), and right ventricular global longitudinal strain (RVGLS) were extracted from text, tables, and graphs. In cases where we believed that multiple articles came from a single dataset, the largest study was selected.

DATA EXTRACTION. All demographic, common clinical characteristics, and strain information were extracted from texts and tables. In cases where the same subjects were measured several times in a day by using the same equipment (7), the first dataset was used. A study applied 2 different software programs to the same population (12). Only the data from 1 software program (TomTec Imaging Systems, Unterschleissheim, Germany) were selected and used because the vast majority of the articles used this software.

OUTCOMES OF INTEREST. In this meta-analysis, our outcomes of interest were normal ranges of LV and RV strains (LVGLS, LVGCS, LVGRS, and RVGLS) measured by MRI-FT.

STATISTICAL ANALYSIS. The means and 95% CIs of LVGLS, LVGCS, LVGRS, and RVGLS were computed using random effects models weighted by inverse variance. Funnel plots with and without the Duval and Tweedie trim and fill were constructed, and the Egger test was used to assess potential publication bias. The heterogeneity between subgroups or between studies was assessed by the Cochran Q test and the inconsistency factor (I^2). Meta-regressions were performed for each risk factor to examine possible study factors associated with heterogeneity. Beta coefficient and its CIs were derived using the least-mean squares fitting method. Statistical analysis was performed using R version 3.2.2 (The R

ABBREVIATIONS AND ACRONYMS

CI = confidence interval

CMR = cardiac magnetic resonance

DENSE = displacement encoding with stimulated echoes

LV = left ventricle/ventricular

LVGCS = left ventricular global circumferential strain

LVGLS = left ventricular global longitudinal strain

LVGRS = left ventricular global radial strain

MRI = magnetic resonance imaging

MRI-FT = magnetic resonance imaging feature tracking

MT = myocardial tagging

RV = right ventricle/ventricular

RVGCS = right ventricular circumferential strain

RVGLS = right ventricular global longitudinal strain

SENC = strain encoding

SSFP = steady-state free precession

STE = speckle tracking echocardiography

JACC: CARDIOVASCULAR IMAGING, VOL. 11, NO. 2, 2018
FEBRUARY 2018:196–205

FIGURE 1 PRISMA Flow Chart

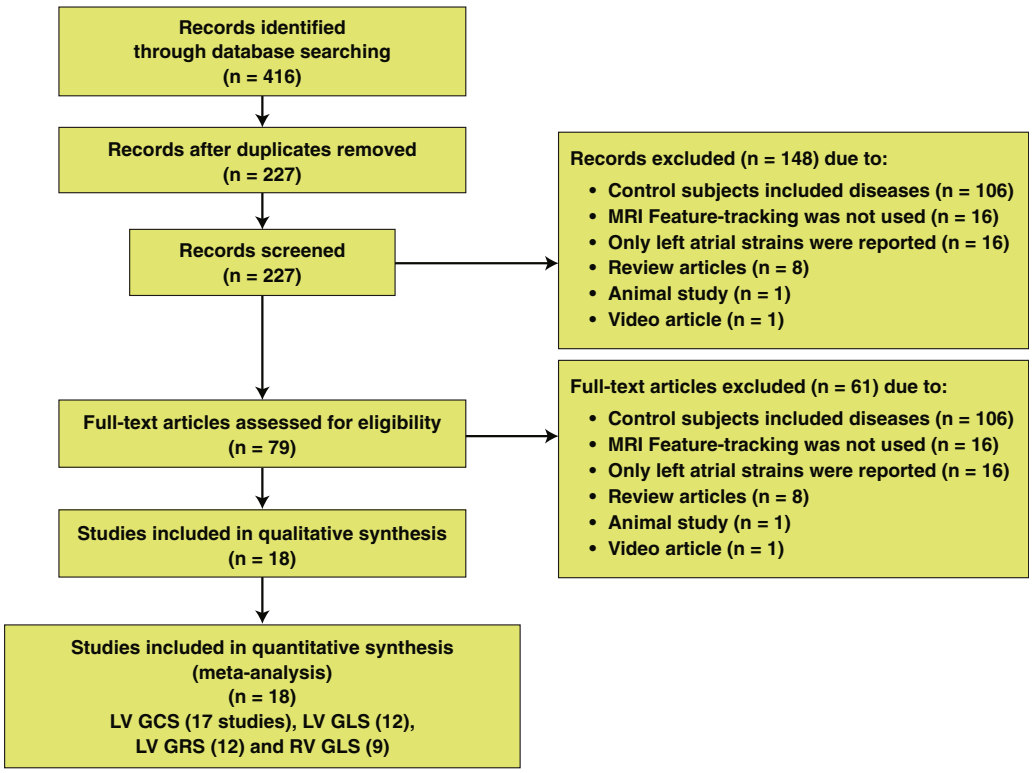

This flow chart illustrates the selection process for published reports on strains by MRI-FT. (The PRISMA flow chart for other MRI-derived strain techniques is presented in Online Figure S4). GCS = global circumferential strain; GLS = global longitudinal strain; GRS = global radial strain; LV = left ventricular; MRI-FT = magnetic resonance imaging feature tracking; RV = right ventricular.

Foundation for Statistical Computing, Vienna, Austria) with the "metafor" package. Two-tailed p values were applied, and the threshold of statistical significance was 0.05 except for the Egger test, where 0.1 was used.

RESULTS

STUDY SELECTION. For MRI-FT, 416 titles were matched with the key terms from the 4 databases (EMBASE [n = 218], PubMed [n = 64], Scopus [n = 59], and Web of Science [n = 75]) (**Figure 1**). Eighteen valid studies (659 normal participants) met the selection criteria and were included in this meta-analysis, where 17 were eligible for LVGCS, 12 for LVGLS and LVGRS, and 9 for RVGLS.

Most subjects were middle-aged (**Table 1**). Many studies (15 of 18 studies) had a small sample size (n ≤ 50), and only 3 studies had a sample size ≥100, with a maximum of 150. Thus, sensitivity analyses were based on the sample size.

Software used for MRI-FT was also collected to find the association of software and the variation of strain. A majority of included studies used software from 1 vendor (Diogenes or 2D CPA, TomTec Imaging Systems), the other software included Velocity Vector Imaging (Siemens Medical Solutions, Malvern, Pennsylvania), Circle (Circle Cardiovascular Imaging, Calgary, Alberta, Canada) (12), and MTT (Toshiba Medical Systems, Tochigi, Japan) (8). Further detailed information can be found in Online Table S2.

NORMAL RANGES OF MRI-FT. LVGLS. The pooled mean of LVGLS was −20.1% (95% CI: −20.9% to −19.3%) (**Figure 2**). Among 12 studies, 9 reported LVGLS from the apical 4-chamber view only and 3 from the 3 apical views, where their values were quite similar. Although no significant publication bias was identified by the funnel plot (Online Figure S1) and the Egger test, there was a significant heterogeneity in LVGLS. A univariable meta-regression was performed to find factors that have significant

TABLE 1 Summary of Included Studies

First Author (Ref. #)	Year	Age, yrs	N	Men	LVEF	Software	Vendor	Strain*	Chamber
Schuster et al. (10)	2011	40.6 (23.9–51.8)	10	5	56.9 ± 4.4	Diogenes	TomTec	L/C/R	LV, RV
Kempny et al. (6)	2012	33.1 ± 15.7	25	15	63.6 ± 5.7	Diogenes	TomTec	L/C/R	LV, RV
Morton et al. (7)	2012	27.9 ± 5.7	16	8	58.5 ± 3.2	Diogenes	TomTec	L/C/R	LV, RV
Li et al. (27)	2012	50 ± 9	14	11	–	VVI	Siemens	C/R	LV
Augustine et al. (17)	2013	29.7 ± 7.6	145	54	–	2D CPA	TomTec	L/C/R	LV
Kutty et al. (28)	2013	37.1 ± 7	20	10	57.5 ± 3.0	2D CPA	TomTec	L/C/R	LV
Padiyath et al. (9)	2013	37 ± 8.5	20	–	–	2D CPA	TomTec	L/C/R	LV, RV
Schuster_1 et al.† (11)	2013	41 (24–52)	10	5	61.3 ± 7.7	Diogenes	TomTec	L/C/R	LV, RV
Schuster_2 et al.† (11)	2013	31 (26–39)	10	5	59 ± 3	Diogenes	TomTec	L/C/R	LV, RV
Orwat et al. (29)	2014	24 ± 3	20	10	64.4 ± 5.3	2D CPA	TomTec	L/C	LV, RV
Wu et al. (30)	2014	37 ± 11	10	9	61 ± 6	Diogenes	TomTec	C	LV
Heermann et al. (5)	2014	24.3 ± 3	10	5	63.6 ± 4.2	Diogenes	TomTec	L	RV
Andre et al. (16)	2015	45.8 ± 14	150	75	–	2D CPA	TomTec	L/C/R	LV
Moody et al. (20)	2015	41 ± 12	33	26	71 ± 6	Diogenes	TomTec	C/R	LV
Nucifora et al. (31)	2015	46 ± 12	15	11	68 ± 8	2D CPA	TomTec	C	LV
Ohyama et al. (8)	2015	53.7 ± 7.5	13	4	66.2 ± 6.5	MTT	Toshiba	L/C	LV, RV
Schuster et al. (12)	2015	40.6 (23–51)	10	5	57.9 ± 5.6	2D CPA	TomTec/Circle	C/R	LV
Taylor et al. (32)	2015	44.5 ± 14	100	50	71.9 ± 6.0	Diogenes	TomTec	L/C/R	LV
Heiberg et al. (33)	2015	21.3 ± 2.5	28	18	56.7 ± 6.2	2D CPA	TomTec	L/C/R	LV

Values are median (interquartile range) or mean ± SD. More detailed information can be found in Online Table S2. *L/C/R = longitudinal/circumferential/radial strain. †This paper reported data from 2 populations.

LV = left ventricle; LVEF = left ventricular ejection fraction; RV = right ventricle; MTT = pixel-based multimodality tissue tracking; VVI = velocity vector imaging.

contributions to the heterogeneity (Online Table S3). LVGLS was not associated with sex, field strength, sequence, scanner vendor, or LV ejection fraction. All studies reported LV GLS used the same software.

LVGCS and LVGRS. The pooled means of LVGCS and LVGRS were −23.0% (95% CI: −24.3% to −21.7%) and 34.1% (95% CI: 28.5% to 39.7%). Among the 17 articles for LVGCS, 10 reported LVGCS from only 1 short-axis level (the papillary muscle level) and the remaining 7 from 3 short-axis levels. Their reported LVGCS values also overlapped (**Figure 3**). Similarly, 7 of 12 reported LVGRS from 1 level only, and the remaining 5 studies, from 3 levels, also showing significant overlap (**Figure 4**).

The Egger tests indicated a publication bias for LVGCS ($p = 0.07$) (Online Figure S1), but not in LVGRS. Normal range in LVGCS from the Duval and Tweedie trim and fill process was quite similar. Sample size was not associated with the LVGCS heterogeneity in both meta-regression, ($\beta = -0.016$; $p = 0.3$) and cumulative forest plot (Online Figure S2). Meta-regression analyses of LVGCS showed significant contributions of field strength (Online Table S3). Among our hypothesized confounding factors, there were no confounders that can significantly explain the heterogeneity of LVGRS.

RVGLS. All 9 studies reported RVGLS from the 4-chamber view only and the pooled mean was −21.8% (95% CI: −23.3% to −20.2%) (**Figure 5**). Although no publication bias was seen, there was significant heterogeneity. In meta-regression analyses, none of age, sex, field strength, sequence, LV ejection fraction, or software vendor was associated with the variability of RVGLS.

Additional analysis. **Table 2** summarizes coefficient of variance of the included articles. LVGCS tends to show smallest interobserver and intraobserver variability in MRI-FT strain.

Subsequent sensitivity analyses based on sample size (all ≥20 or ≥100) revealed no obvious effect of sample size (Online Figure S3). Additional sensitivity analyses limiting articles using TomTec software showed similar results (Online Table S4).

Similar investigations were performed for SENC, DENSE, and MT. Results are summarized in **Table 3** and Online Figures S4 to S7, and Online Tables S5 to S8. MRI-FT and SENC share similar LVGLS, but MT showed smaller. MRI-FT demonstrated slightly larger LVGCS than the other MRI strain techniques. There were substantial heterogeneities in normal ranges of LVGRS and RVGLS.

DISCUSSION

This is the first systematic review and meta-analysis, to our knowledge, of pooled mean of MRI-FT among normal subjects. Although MRI-FT has substantial potential, the normal ranges from the 2 largest studies have no overlaps. This really

FIGURE 2 LVGLS in Normal Subjects

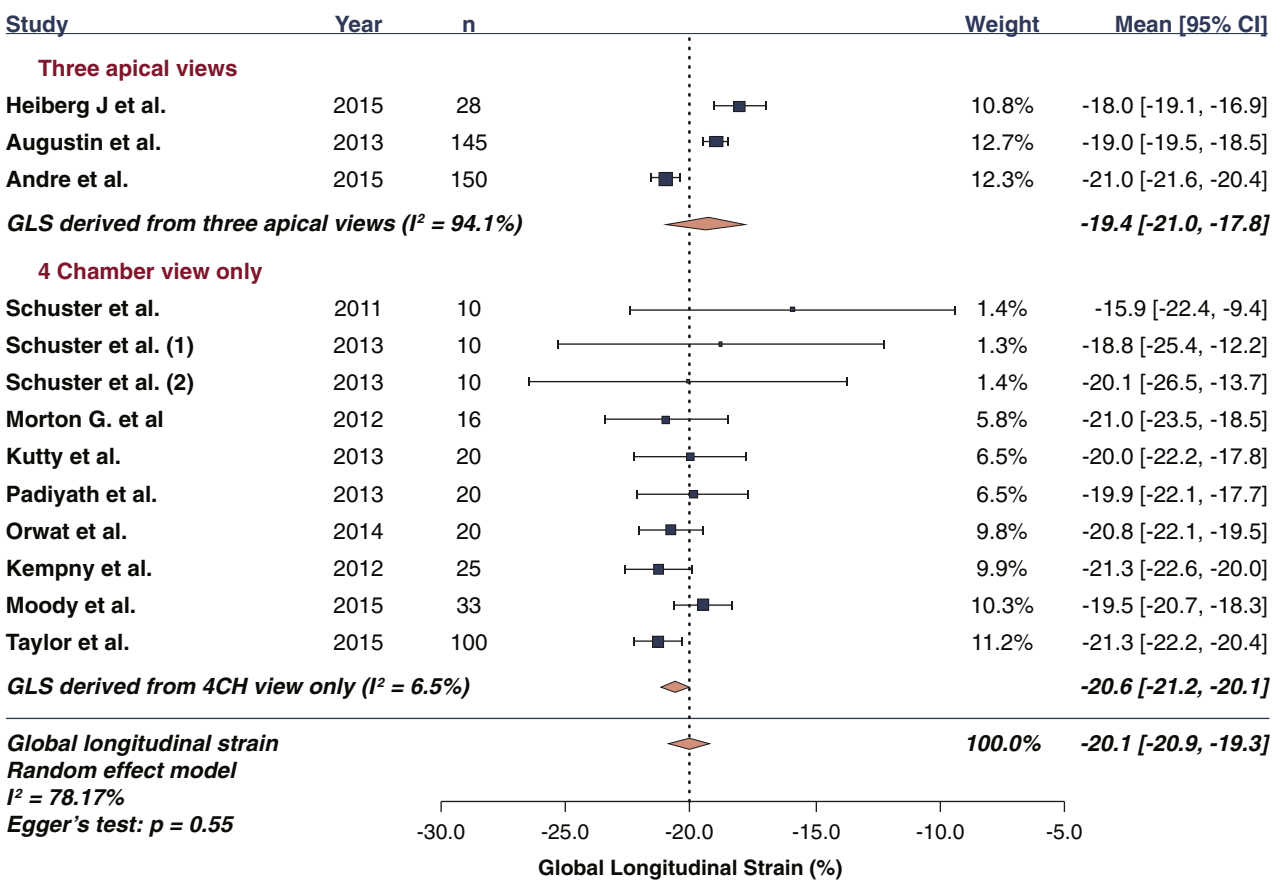

Forest plot divided by methods of calculation: **(top)** GLS from 3 apical views, and **(bottom)** GLS from 4-chamber (4CH) view only. CI = confidence interval; other abbreviations as in Figure 1.

hampers wider use of this technique. Our results warrant the need for a larger-scale study determining normal ranges for FT strains, preferably with some standardizations for the number of views used. In the meantime, estimated means (with 95% CI) would serve as a reasonable guide for end users. We also performed similar analyses for other MRI-derived strains such as MT, SENC, and DENSE as comparators.

SOFTWARE. Software from 1 vendor dominated currently, and more than one-half of the studies measured LV strains from a single view, but this had a minimal impact on these measurements. Most articles used steady-state free precession (SSFP) or balanced SSFP cine images (Online Table S1). The main reasons for this are: 1) a routine CMR technique; 2) high contrast-to-noise ratio at the endocardial-blood interface; 3) little blood flow dependency; 4) higher temporal resolution; and 5) short acquisition time (8). The other sequence used was fast gradient echo cine (8). Their strain values were similar to those from SSFP but required a longer acquisition time.

SAMPLE SIZE. Most of studies included had a small sample size ($n \leq 50$), and only 3 studies had sample size ≥100, with a maximum of 150, with limited overlap among their normal ranges. This may be because CMR requires more resources than other noninvasive cardiac modalities. LVGLS was minimally affected by the sample sizes. LVGCS from small-sized studies seemed to show smaller values, although this was not a significant determinant of LVGCS in the meta-regression.

SLICES. More than one-half of the studies derived LVGCS and LVGRS from a single slice at the papillary muscle level only, and the rest used 3 short-axis planes although their normal ranges overlapped

FIGURE 3 LVGCS in Normal Subjects

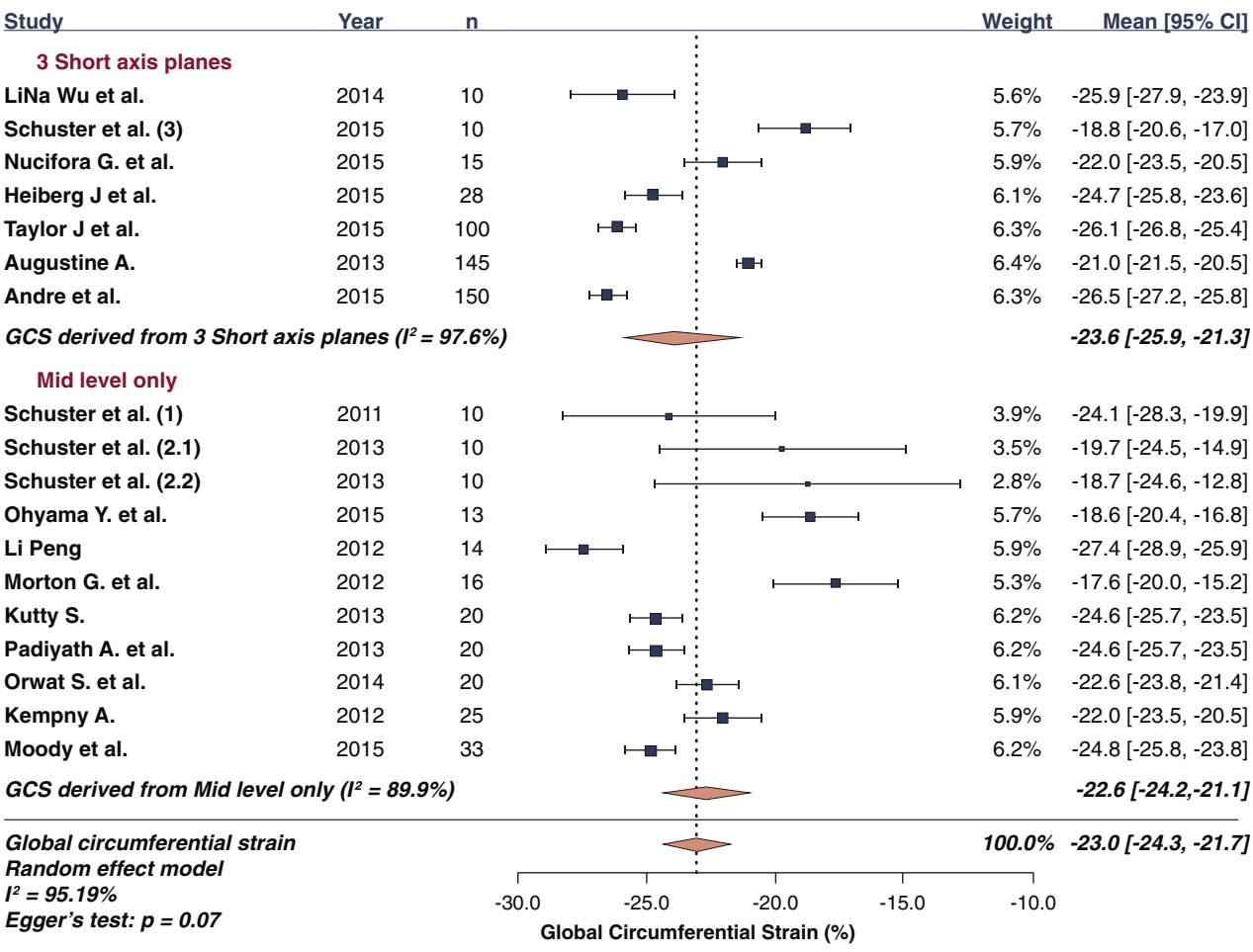

Forest plot divided by methods of calculation: **(top)** GCS from 3 levels of short-axis planes, and **(bottom)** GCS only from the mid-ventricular plane. Abbreviations as in Figures 1 and 2.

(Figures 3 and 4). Similarly, most of the LVGLS were calculated from the 4-chamber view only, whereas only 3 papers used 3 apical views. They are also overlapped (Figure 2). Nevertheless, the use of a single-plane method should depend on the underlying disease: if a heterogeneous distribution of disease process can be anticipated, the 3-level method would reflect more accurate deformation of the whole heart.

OBSERVER VARIABILITY. Although the normal values of LVGLS and LVGCS fluctuated in a narrow range, LVGRS had a wider range of CIs. Online Figure S3 also reflects this variation, where LVGRS for different sample sizes yielded an unpredictable pattern. Unfortunately, our meta-regression analyses did not identify the source of this variation. The same issue has been reported in STE (19), and its causes remain contentious. We speculate that through-plane motion could be a partial explanation for this problem.

CALCULATION OF GLOBAL STRAIN. Another point to be mentioned is that there are 2 ways of calculating global strain: 1) an average of the peaks of individual strain curves; and 2) peak of the mean curve. Only 1 paper clarified which method was used to obtain global strains. Although a high correlation between the 2 methods was reported (16), this ambiguity caused difficulties and bias in this meta-analysis. In this context, only results from the second method were included. In addition, a few studies measured

FIGURE 4 LVGRS in Normal Subjects

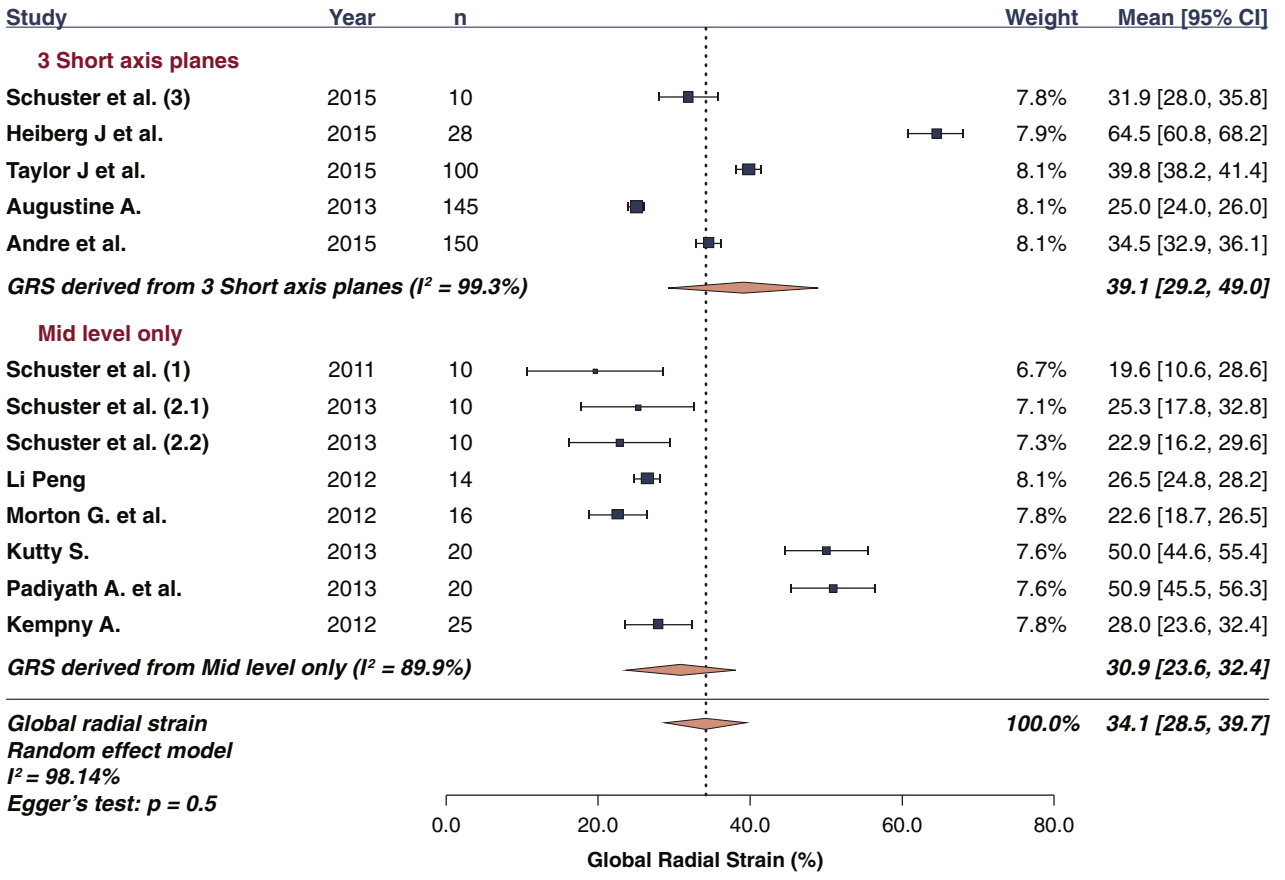

Forest plot divided by methods of calculation: **(top)** GRS from 3 levels of short-axis planes, and **(bottom)** GRS only from mid-ventricular plane. Abbreviations as in Figures 1 and 2.

LVGLS using 3 apical views and LVGCS and LVGRS from 3 short-axis planes.

HETEROGENEITY AMONG STUDIES. In our meta-analysis, each of the strain metrics had large I^2 values. The interpretation of I^2 is discussed in Online Appendix F. Most of our hypothesized confounding factors were not fully explanatory for this. This problem could be further explained by 3 potential reasons: 1) Population. Normal strain values among different populations may slightly differ. 2) Interobserver variability. Interobserver variability could be another source of variation among studies. Differences defining myocardial contours may result in between-study heterogeneity. Table 2 summarizes inter-observer and intraobserver variability of included studies. The coefficients of variation of the inter-observer variability ranged from 3.7% to 32.2%, whereas those of intraobserver variability were 2.7% to 43.5%. LVGCS seems to be the most robust. 3) Different software vendors also could be a source of heterogeneity. However, our sensitivity analysis including studies using TomTec only (Online Tables S4a and S4b) did not show substantial reduction in I^2.

COMPARISONS WITH NORMAL RANGES AMONG VARIOUS METHODS. Normal ranges of STE, MT, SENC, DENSE, and MRI-FT are summarized in Table 3. Although MRI-FT-derived LVGLS and LVGCS yield quite similar ranges to those of STE, there are discrepancies in LVGRS and RVGLS.

MT is an MRI technique that generates grid patterns or parallel lines on the magnitude-reconstructed images (spatial modulation of magnetization [SPAMM] or complementary SPAMM [CSPAMM]), which are then analyzed, or by extracting information about myocardial tags in k-space (harmonic phase imaging [HARP]). The strength of

FIGURE 5 RVGLS in Normal Subjects

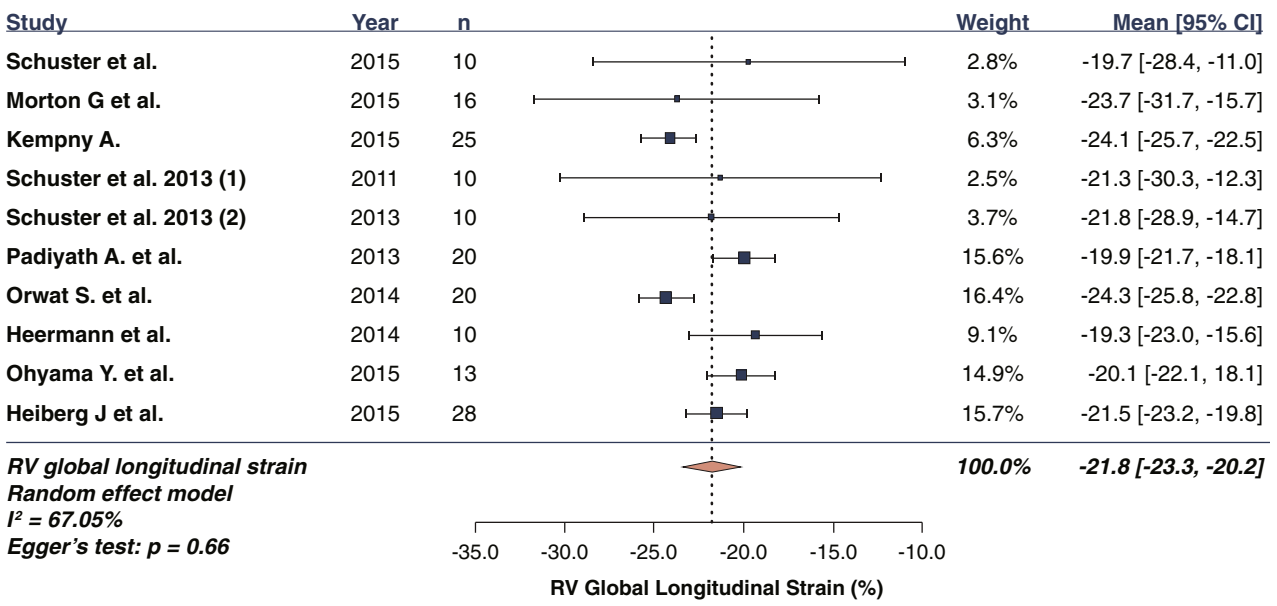

Forest plot of RVGLS. Abbreviations as in Figures 1 and 2.

MT is its insensitivity to through-plane motion (17). However, MT suffers a low temporal resolution, low signal-noise ratio, and requires some extra sequences, prolonged image acquisition, and a longer breath-hold. The agreement between MRI-FT and MT still remains controversial. Some reported a poor agreement (20), others showed high correlations (17,21). In this study, LVGLS and LVGCS by MT were somewhat less negative than those by STE and MRI-FT. This could be due to its insensitivity to through-plane motion.

DENSE is another technique for strain calculation, first introduced in 1999 (22). The phase-reconstructed images by DENSE have high temporal and spatial resolution, and direct extraction of motion data (23,24). However, this technique requires some specific sequences, which may prolong scan time. So far, applications of DENSE in clinical practice have been still limited by small sample size and only applied for short-axis images. The pooled normal ranges of DENSE were lower than MRI-FT. Due to a few studies that

TABLE 2 A Summary of Interobserver and Intraobserver Variabilities of Included Studies, Expressed as Coefficient of Variance

First Author/Year (Ref. #)	Intraobserver				Interobserver			
	LVGLS	LVGCS	LVGRS	RVGLS	LVGLS	LVGCS	LVGRS	RVGLS
Kempny et al., 2012 (6)	10.8	6.7	21.4	9.7	9.6	8.5	21.4	8.3
Schuster et al., 2011 (10)	–	3.7	9.9	–	–	3.7	9.9	–
Augustine et al., 2013 (17)	12.3	2.8	22.9	–	10.9	4.9	32.2	–
Schuster et al., 2013, 1.5-T (11)	17.3	13.3	16.4	28.7	–	–	–	–
Schuster et al., 2013, 3-T (11)	18.1	17.2	19.8	43.5	–	–	–	–
Orwat et al., 2014 (29)	–	–	–	–	13.2	11.1	–	–
Andre et al., 2015 (16)	4.3	4.8	7.9	–	4.8	5.7	10.0	–
Taylor et al., 2015 (32)	7.68	3.55	8.9	–	5.48	4.95	14.67	–
Schuster et al., 2015 (12)	–	2.69	10.1	–	–	4.4	13.2	–

Values are %.

LVGCS = left ventricular global circumferential strain; LVGLS = left ventricular global longitudinal strain; LVGRS = left ventricular global radial strain; RVGLS = right ventricular global longitudinal strain.

TABLE 3 Comparison Between DENSE, SENC, MT, STE, and MRI-FT in Normal Strain Values

	SENC	DENSE	Tagging	Feature Tracking	Speckle Tracking*
LVGLS	−20.0 (−22.5 to −17.4)	–	−14.6 (−16.2 to −12.9)	−20.1 (−20.9 to −19.3)	−19.7 (−20.4 to −18.9)
LVGCS	−20.9 (−22.4 to −19.3)	−19.0 (−19.7 to −18.3)	−19.9 (−21.1 to −17.7)	−23.0 (−24.3 to −21.7)	−23.3 (−24.6 to −22.1)
LVGRS	–	24.3 (16.2 to 32.3)	–	34.1 (28.5 to 39.7)	47.3 (43.6 to 51.0)
RVGLS	−18.7 (−19.5 to −17.9)	–	–	−21.8 (−23.3 to −20.2)	−27.0 (−29.0 to −24.0)
RVGCS	−19.3 (−21.2 to −17.4)	–	–	–	–

Values are mean (95% confidence interval). *Adapted with permission from Yingchoncharoen et al. (20).

DENSE = displacement encoding with stimulated echoes; MRI-FT = magnetic resonance imaging feature tracking; MT = myocardial tagging; RVGCS = right ventricular global circumferential strain; SENC = strain encoding; STE = speckle tracking echocardiography; other abbreviations as in Table 2.

reported LVGRS by DENSE, 95% CI varied in a very wide range.

SENC is developed on the concepts of myocardial MT, but it uses tag planes parallel to the image plane (25). In other words, LVGLS is obtained from short-axis views, and LVGCS from long-axis views. In general, normal ranges of SENC were similar to those by MRI-FT. Interestingly, SENC can provide right ventricular global circumferential strain (RVGCS). Between-study variability of both LVGCS and RVGCS by SENC could be explained by the proportions of males. Additionally, that of RVGCS could be also explained by age, sex, and software vendors.

STUDY LIMITATIONS. Several factors merit consideration in the interpretation of our results. First, like all meta-analyses, this work is limited by variations in the original studies and publication bias, although we followed standard approaches to detect this. Likewise, the constituent observational studies may be limited by biases in the recruitment process. Second, we have assumed that all of the measurements were performed by experts, but the levels of expertise among individuals who have actually measured the strain are uncertain. Third, significant heterogeneities among studies were identified. Thus, we performed subsequent meta-regression analyses and stratifications to elucidate the sources of the variations. Fourth, as mentioned earlier in the text, most papers had sample sizes of <50, and studies with larger sample sizes are needed for a more accurate estimation of normal ranges in MRI-FT, especially in RVGLS. Fifth, our study may not have enough power to test vendor differences because only 3 studies reported non-TomTec software data. Only 1 MRI-FT study performed a head-to-head comparison (12). Further studies on this issue should be warranted because this could be a modifiable issue as shown in STE (26). Sixth, the high intrastudy and interstudy variability, and the systematic differences between studies cause difficulties in deriving clear normal ranges. Finally, strain is affected by loading conditions, but we had insufficient data to analyze this.

CONCLUSIONS

The pooled means of MRI-FT strains are similar to those of STE. Differences in sequence and software were attributed to variations of LVGRS and LVGCS, respectively. LVGLS and RVGLS variations seemed likely not to be attributed to any of age, sex, software, field strength, or sequence.

ACKNOWLEDGMENT The authors thank Ms. Elizabeth Seymour for her support in systematic review.

ADDRESS FOR CORRESPONDENCE: Dr. Kazuaki Negishi, Menzies Institute for Medical Research, University of Tasmania, 17 Liverpool Street, Private Bag 23, Hobart, 7000, Australia. E-mail: Kazuaki.Negishi@utas.edu.au.

PERSPECTIVES

COMPETENCY IN MEDICAL KNOWLEDGE: Reported 95% CIs from the 2 largest studies on normal ranges of MRI-based feature tracking strain have no overlaps. The pooled means of myocardial strain in normal subjects are demonstrated via systematic review and meta-analysis in 4 different MRI-derived methods (MRI-based feature tracking, strain encoding, displacement encoding with stimulated echoes, and myocardial tagging).

TRANSLATIONAL OUTLOOK: Although MRI-based feature tracking strain has substantial potential, our results warrant the need for a larger-scale study determining normal rages, preferably with some methodological standardizations including the number of views used. In the meantime, estimated means in MRI-based strain methods would serve as a reasonable guide for end users.

REFERENCES

1. Negishi K, Negishi T, Hare JL, Haluska BA, Plana JC, Marwick TH. Independent and incremental value of deformation indices for prediction of trastuzumab-induced cardiotoxicity. J Am Soc Echocardiogr 2013;26:493–8.

2. Negishi K, Negishi T, Haluska BA, Hare JL, Plana JC, Marwick TH. Use of speckle strain to assess left ventricular responses to cardiotoxic chemotherapy and cardioprotection. Eur Heart J Cardiovasc Imaging 2014;15:324–31.

3. Attili AK, Schuster A, Nagel E, Reiber JH, van der Geest RJ. Quantification in cardiac MRI: advances in image acquisition and processing. Int J Cardiovasc Imaging 2010;26 Suppl 1:27–40.

4. Harrild DM, Han Y, Geva T, Zhou J, Marcus E, Powell AJ. Comparison of cardiac MRI tissue tracking and myocardial tagging for assessment of regional ventricular strain. Int J Cardiovasc Imaging 2012;28:2009–18.

5. Heermann P, Hedderich DM, Paul M, et al. Biventricular myocardial strain analysis in patients with arrhythmogenic right ventricular cardiomyopathy (ARVC) using cardiovascular magnetic resonance feature tracking. J Cardiovasc Magn Reson 2014;16:75.

6. Kempny A, Fernández-Jiménez R, Orwat S, et al. Quantification of biventricular myocardial function using cardiac magnetic resonance feature tracking, endocardial border delineation and echocardiographic speckle tracking in patients with repaired tetralogy of Fallot and healthy controls. J Cardiovasc Magn Reson 2012;14:32.

7. Morton G, Schuster A, Jogiya R, Kutty S, Beerbaum P, Nagel E. Inter-study reproducibility of cardiovascular magnetic resonance myocardial feature tracking. J Cardiovasc Magn Reson 2012;14:43.

8. Ohyama Y, Ambale-Venkatesh B, Chamera E, et al. Comparison of strain measurement from multimodality tissue tracking with strain-encoding MRI and harmonic phase MRI in pulmonary hypertension. Int J Cardiol 2015;182:342–8.

9. Padiyath A, Gribben P, Abraham JR, et al. Echocardiography and cardiac magnetic resonance-based feature tracking in the assessment of myocardial mechanics in tetralogy of Fallot: an intermodality comparison. Echocardiography 2013;30:203–10.

10. Schuster A, Kutty S, Padiyath A, et al. Cardiovascular magnetic resonance myocardial feature tracking detects quantitative wall motion during dobutamine stress. J Cardiovasc Magn Reson 2011;13:58.

11. Schuster A, Morton G, Hussain ST, et al. The intra-observer reproducibility of cardiovascular magnetic resonance myocardial feature tracking strain assessment is independent of field strength. J Cardiovasc Magn Reson 2013;15:12.

12. Schuster A, Stahnke VC, Unterberg-Buchwald C, et al. Cardiovascular magnetic resonance feature-tracking assessment of myocardial mechanics: intervendor agreement and considerations regarding reproducibility. Clin Radiol 2015;70:989–98.

13. Habibi M, Lima JA, Khurram IM, et al. Association of left atrial function and left atrial enhancement in patients with atrial fibrillation: cardiac magnetic resonance study. Circ Cardiovasc Imaging 2015;8:e002769.

14. Kowallick JT, Kutty S, Edelmann F, et al. Quantification of left atrial strain and strain rate using Cardiovascular Magnetic Resonance myocardial feature tracking: a feasibility study. J Cardiovasc Magn Reson 2014;16:60.

15. Jeung MY, Germain P, Croisille P, El ghannudi S, Roy C, Gangi A. Myocardial tagging with MR imaging: overview of normal and pathologic findings. Radiographics 2012;32:1381–98.

16. Andre F, Steen H, Matheis P, et al. Age- and gender-related normal left ventricular deformation assessed by cardiovascular magnetic resonance feature tracking. J Cardiovasc Magn Reson 2015;17:25.

17. Augustine D, Lewandowski AJ, Lazdam M, et al. Global and regional left ventricular myocardial deformation measures by magnetic resonance feature tracking in healthy volunteers: comparison with tagging and relevance of gender. J Cardiovasc Magn Reson 2013;15:8.

18. Moher D, Liberati A, Tetzlaff J, Altman DG, PRISMA Group. Preferred reporting items for systematic reviews and meta-analyses: the PRISMA Statement. Open Med 2009;3:e123–30.

19. Yingchoncharoen T, Agarwal S, Popović ZB, Marwick TH. Normal ranges of left ventricular strain: a meta-analysis. J Am Soc Echocardiogr 2013;26:185–91.

20. Moody WE, Taylor RJ, Edwards NC, et al. Comparison of magnetic resonance feature tracking for systolic and diastolic strain and strain rate calculation with spatial modulation of magnetization imaging analysis. J Magn Reson Imaging 2015;41:1000–12.

21. Hor KN, Gottliebson WM, Carson C, et al. Comparison of magnetic resonance feature tracking for strain calculation with harmonic phase imaging analysis. J Am Coll Cardiol Intv 2010;3:144–51.

22. Aletras AH, Ding S, Balaban RS, Wen H. DENSE: displacement encoding with stimulated echoes in cardiac functional MRI. J Magn Reson 1999;137:247–52.

23. Kim D, Gilson WD, Kramer CM, Epstein FH. Myocardial tissue tracking with two-dimensional cine displacement-encoded MR imaging: development and initial evaluation. Radiology 2004;230:862–71.

24. Mangion K, Clerfond G, McComb C, et al. Myocardial strain in healthy adults across a broad age range as revealed by cardiac magnetic resonance imaging at 1.5 and 3.0T: Associations of myocardial strain with myocardial region, age, and sex. J Magn Reson Imaging 2016;44:1197–205.

25. Osman NF, Sampath S, Atalar E, Prince JL. Imaging longitudinal cardiac strain on short-axis images using strain-encoded MRI. Magn Reson Med 2001;46:324–34.

26. Yang H, Marwick TH, Fukuda N, et al. Improvement in strain concordance between two major vendors after the strain standardization initiative. J Am Soc Echocardiog 2015;28:642–8.e7.

27. Li P, Meng H, Liu SZ, Vannan MA. Quantification of left ventricular mechanics using vector-velocity imaging, a novel feature tracking algorithm, applied to echocardiography and cardiac magnetic resonance imaging. Chin Med J (Engl) 2012;125:2719–27.

28. Kutty S, Rangamani S, Venkataraman J, et al. Reduced global longitudinal and radial strain with normal left ventricular ejection fraction late after effective repair of aortic coarctation: a CMR feature tracking study. Int J Cardiovasc Imaging 2013;29:141–50.

29. Orwat S, Kempny A, Diller GP, et al. Cardiac magnetic resonance feature tracking: a novel method of assessing myocardial strain. Comparison with echocardiographic speckle tracking in healthy volunteers and in patients with left ventricular hypertrophy. Kardiol Pol 2014;72:363–71.

30. Wu LN, Germans T, Guclu A, Heymans MW, Allaart CP, van Rossum AC. Feature tracking compared with tissue tagging measurements of segmental strain by cardiovascular magnetic resonance. J Cardiovasc Magn Reson 2014;16:10.

31. Nucifora G, Muser D, Gianfagna P, Morocutti G, Proclemer A. Systolic and diastolic myocardial mechanics in hypertrophic cardiomyopathy and their link to the extent of hypertrophy, replacement fibrosis and interstitial fibrosis. Int J Cardiovasc Imaging 2015;31:1603–10.

32. Taylor RJ, Moody WE, Umar F, et al. Myocardial strain measurement with feature-tracking cardiovascular magnetic resonance: normal values. Eur Heart J Cardiovasc Imaging 2015;16:871–81.

33. Heiberg J, Ringgaard S, Schmidt MR, Redington A, Hjortdal VE. Structural and functional alterations of the right ventricle are common in adults operated for ventricular septal defect as toddlers. Eur Heart J Cardiovasc Imaging 2015;16:483–9.

KEY WORDS DENSE, feature tracking, healthy, magnetic resonance, meta-analysis, normal range, SENC, strain, tagging

APPENDIX For an expanded Methods section, and supplemental figures and tables, please see the online version of this paper.